NAWCWD TP 8673
NAVAIR

Application of Numerical Methods To Solve Integral Equations Arising in Computational Physics/Electromagnetics

by
Elizabeth Yuhas
Physics and Computational Sciences Department

AUGUST 2009

NAVAL AIR WARFARE CENTER WEAPONS DIVISION
CHINA LAKE, CA 93555-6100

Naval Air Warfare Center Weapons Division

FOREWORD

This document describes an effort conducted to devise basic models to analyze fundamental electrostatic and electrodynamics problems. Through the use of numerical methods and Matlab, the author modeled parts of problems that are difficult to solve without numerical integration. This report describes how she used the method of moments as an approach to solve integral equations in electrostatic and electrodynamics problems.

Approved by
R. NISSAN, *Head*
Research and Intelligence Department
28 August 2009

Under authority of
M. G. STORCH
CAPT, U.S. Navy
Commander (Acting)

Released for publication by
S. O'NEIL
Director for Research and Engineering

NAWCWD Technical Publication 8673

Published by .... Technical Communication Office
Collation.. Cover, 13 leaves
First printing .... 22 paper, 2 electronic

REPORT DOCUMENTATION PAGE

Form Approved
OMB No. 0704-0188

1. REPORT DATE *(DD-MM-YYYY)*	2. REPORT TYPE	3. DATES COVERED *(From - To)*
28-08-2009	Summary	June 2008–January 2009

4. TITLE AND SUBTITLE

Application of Numerical Methods To Solve Integral Equations Arising in Computational Physics/Electromagnetics(U)

5a. CONTRACT NUMBER

5b. GRANT NUMBER

5c. PROGRAM ELEMENT NUMBER

6. AUTHOR(S)

Elizabeth Yuhas

5d. PROJECT NUMBER

5e. TASK NUMBER

5f. WORK UNIT NUMBER

7. PERFORMING ORGANIZATION NAME(S) AND ADDRESS(ES)

Naval Air Warfare Center Weapons Division
China Lake, CA 93555-6100

8. PERFORMING ORGANIZATION REPORT NUMBER

NAWCWD TP 8673

9. SPONSORING / MONITORING AGENCY NAME(S) AND ADDRESS(ES)

Naval Air Warfare Center Weapons Division
China Lake, CA 93555-6100

10. SPONSOR/MONITOR'S ACRONYM(S)

11. SPONSOR/MONITOR'S REPORT NUMBER(S)

12. DISTRIBUTION / AVAILABILITY STATEMENT

Approved for public release; distribution is unlimited.

13. SUPPLEMENTARY NOTES

14. ABSTRACT

(U) The author, as part of an internship under the Joint Educational Opportunities for Minorities (JEOM) Program at Naval Air Warfare Center Weapons Division (NAWCWD), China Lake, California, has devised models and methods for the solution of certain frequently recurring problems in electrical engineering. Starting with fundamental equations relating to line charges, the author utilizes the well-known method of moments to model single strip charges, multiple strip charges in various geometrical configurations, and a charged square cylinder excited by an incidental plane wave. Finally, the author considers the problem of calculating the current along a thin-wire antenna.

15. SUBJECT TERMS

Numerical Methods, Method of Moments, Pulse Functions, Electric Field Integral Equation, Hallén's Integral Equation, Electrical Engineering, Electrostatics, Electrodynamics, Line Charges, Strip Charges, Transverse Magnetic Illumination, Thin-wire Antenna

16. SECURITY CLASSIFICATION OF:			17. LIMITATION OF ABSTRACT	18. NUMBER OF PAGES	19a. NAME OF RESPONSIBLE PERSON
					Klaus Halterman
a. REPORT	b. ABSTRACT	c. THIS PAGE	SAR	24	19b. TELEPHONE NUMBER *(include area code)*
UNCLASSIFIED	UNCLASSIFIED	UNCLASSIFIED			(760) 939-6543

Standard Form 298 (Rev. 8-98)
Prescribed by ANSI Std. Z39.18

CONTENTS

INTRODUCTION

The author, as part of her Joint Educational Opportunities for Minorities (JEOM) internship through the Department of Defense under the cognizance of Klaus Halterman of the Naval Air Warfare Center Weapons Division (NAWCWD), China Lake, California, has undertaken learning computational physics/electromagnetics in order to devise basic models to analyze fundamental problems. Through the use of numerical methods and Matlab, the author modeled parts of problems that are difficult to solve without numerical integration. This technical publication describes how she used the method of moments as an approach to solve integral equations in electrostatic and electrodynamics problems.

Line charges are very fundamental electrostatic problems. By modeling the effect of all the charges in the area surrounding the line, analysts can get an idea of the electric field around the line. Taking this approach one step further, they are able to apply similar concepts to the strip problem. This problem is set up as a strip of metal that has a specific width, is infinitely long, and is infinitesimally thin, a configuration that can be thought of as a group of line charges all lying next to each other. By applying a potential to the strip, analysts attempt to calculate the charge density across the strip. In the equations that are used, the charge density values are part of the integral, thereby making it necessary to use an alternate method of numerical integration. For this task, the author used the method of moments. Herein, the strips are divided into pulses and pulse points, and pulse matching is performed to approximate the actual result. As such, the more pulses that are used, the more accurate the results are, to a certain extent. In this method, the unknown variable becomes a summation of unknown constants multiplied by measurable values and can, therefore, be removed from the integral. By solving the problem like a set of equations using matrices, the author was able to find the values of the unknown constants and thereby determine the charge density at the pulse points across the strip. The author was able to graph the charge density across the strip and see the differences when different forcing functions were used, as well as when the number of pulse points were increased.

The author applied the same method for alternate setups of the strip problems, including coupled strips aligned linearly, coupled strip in a cylinder, and a square-cylinder electrodynamics problem. The square-cylinder problem was slightly different because the cylinder was excited by an incident plane wave normal to the cylinder axis. As a consequence, a transverse magnetic scattering problem resulted. It was approached the same way as the other strip problems, but with a different formula for the forcing function. The author was able to look at the current density around the square cylinder and at the charge density in the coupled strip problems.

The author examined a thin-wire antenna problem, which she approached in a very similar way as the strip problem, but used a different set of equations. The author was able to look at the effect of different lengths of the antenna, different radii, and different feed locations. She also changed the forcing function from a delta function excitation to an incidental plane wave, thereby generating a scattering problem. Therein, she looked at the change in the length of the antenna.

LINE CHARGES

In basic electrostatics, a line charge is a source charge spread out along a line of an inconsequentially small radius, which essentially acts as a line of infinitesimally small point charges. The formula for calculating the electric field due to the line charges is based on the formula for point charges (Equation 1).

$$E\left(P\right)=\frac{1}{4\pi\,\varepsilon_0}\sum_{i=1}^{n}\frac{q_i}{r_i^{\,2}}\hat{r}_i \tag{1}$$

This formula provides the electric field, E, generated by the charges $q_1, \ldots, q_n$ acting on point P. where ε_0 (8.854223×10^{-12} Farads/meter) is the permittivity of free space, $\hat{r}$ is the unit vector between the point P and the source charge q_i, and r is the distance between the point P and the source charge q_i. Breaking the line into infinitely many small pieces, each of length dl, and calculating the charge at each small piece result in the integral equation (Equation 2).

$$E\left(P\right)=\frac{1}{4\pi\,\varepsilon_0}\int_{line}\frac{\hat{r}_i}{r_i^{\,2}}\lambda\,dl \tag{2}$$

Herein, $\hat{r}$ is the unit vector between dl and P; r is the distance between dl and P; and λ represents the charge per unit length (dq/dl), which is a constant.

Figure 1 shows how the results of the equation change when the distance varies along the y-axis. As the data points indicate, an inverse relationship exists between the distance for the line and the voltage level. For example, as the distance from the line decreases, the voltage increases, and vice versa.

Figure 2 is a two-dimensional plot of the field strength around the line charge. The charge through the 10-meter line is uniformly distributed, and $\lambda = 5$. Herein, the distance can be varied in both the x and y directions. This figure shows the same inverse relationship between the distance from the line and the voltage mentioned earlier.

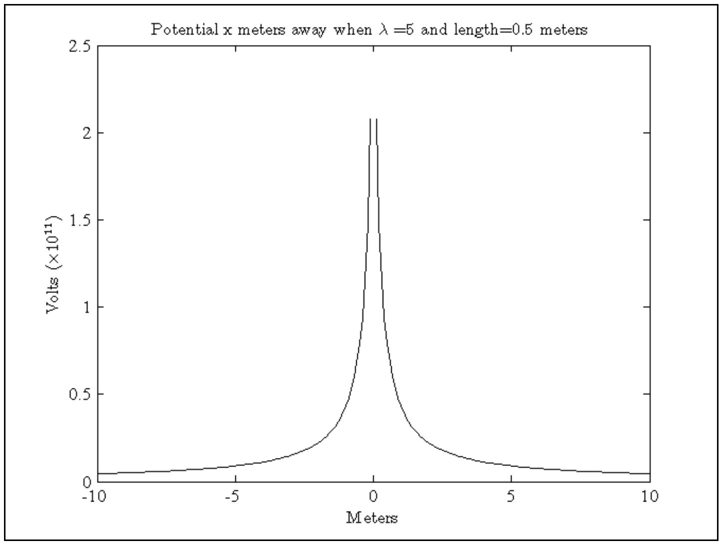

FIGURE 1. Line Charge Problem Results, Voltage vs. Distance From Line. The line charge was centered at x = 0, and the distances were varied only in the y direction.

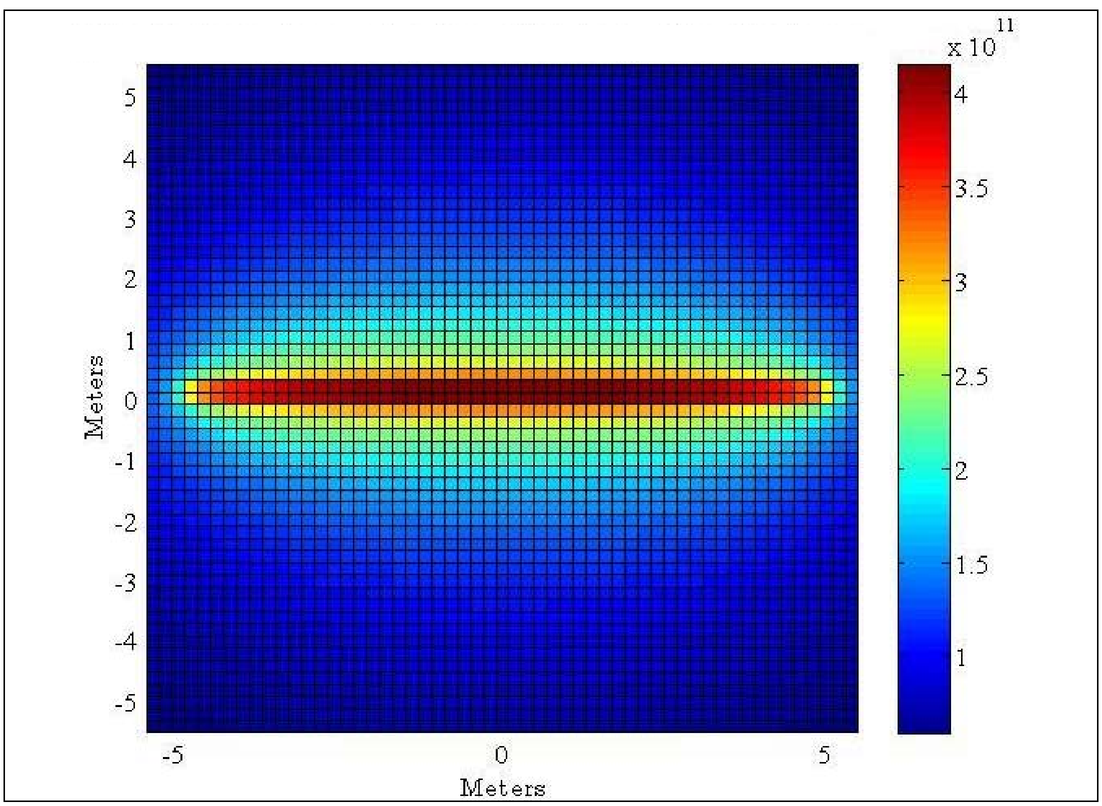

FIGURE 2. Two-dimensional Plot of Field Strength Around 10-meter Line Charge.

USING METHOD OF MOMENTS IN STRIP PROBLEM

This problem involves an infinitesimally thin, infinitely long strip of material that is of a given width, centered along the y-axis, and has a given potential applied across its surface. The equation for this problem is based on the equation for the potential of a line charge (Equation 3).

$$d\phi(\vec{\rho}) = \frac{q_L}{2\pi\,\varepsilon_0}\ln\left(\frac{1}{\left|\vec{\rho} - \dot{\vec{\rho}}\right|}\right) \tag{3}$$

Herein, $d\phi$ is the electric potential, $\vec{\rho}$ is the location at which the potential is observed, q_L is the line charge density, ε_0 again is a constant (8.854223×10^{-12} Farads/meter), and $\dot{\vec{\rho}}$ is the location of the charge.

The charge density across the strip changes in neither the y nor the z direction because of its specific dimensions: infinitesimally thin in the z direction and infinitely long in the y direction. As a result, only the x direction is considered when calculating the charge density, and the vector quantities $\vec{\rho}$ and $\dot{\vec{\rho}}$ may be reduced to their scalar x-components, x and $\dot{x}$. The charge density is found by multiplying the surface density, $q_s(\dot{x})$, by the differential change in $\dot{x}$ (Equation 4).

$$q_L(\dot{x}) = q_s(\dot{x})\,d\dot{x} \tag{4}$$

Placing this equation into Equation 3 and integrating both sides results in Equation 5.

$$\Phi(x) = \int_{(-\delta/2)}^{(\delta/2)} \frac{q_s(\dot{x})}{2\pi\,\varepsilon_0}\ln\frac{1}{\left|x - \dot{x}\right|}\,d\dot{x} \tag{5}$$

Herein, Φ(x) is the forcing function and δ is the width of the strip.

The method of moments is used to solve for $q_s(\dot{x})$ to circumvent the difficulties that arise when solving for a variable in an integrand in a standard way. The first step is to divide the width of the strip into N divisions of δ/N size. In this method, only $q_s(\dot{x})$ at the center of the sections is measured and that measurement is utilized for the whole section (see Figure 3). This method involves using pulse expansion, wherein the pulse function is integrated into the integral through a summation.

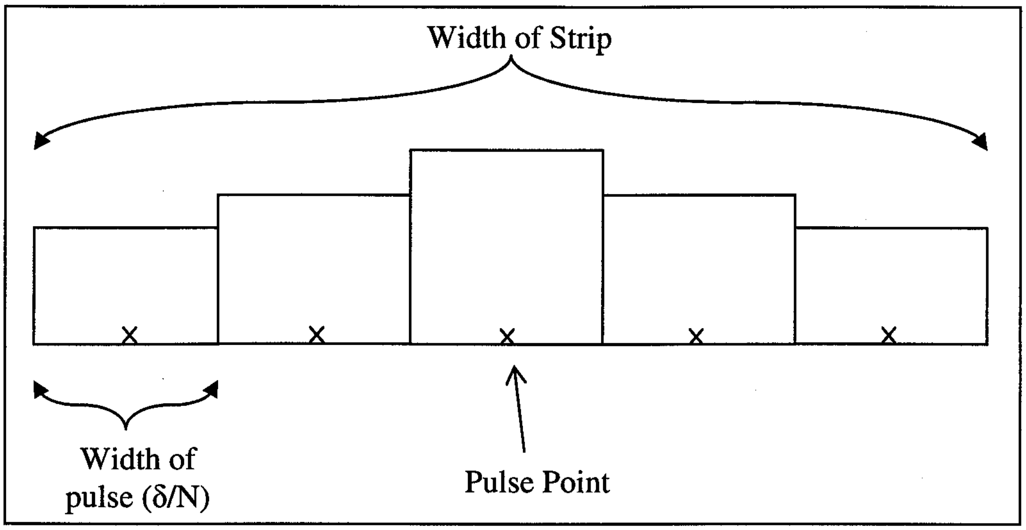

FIGURE 3. Pulse Expansion.

The pulse expansion function is defined as Equation 6.

$$q(x) = q_s(\dot{x}) \approx \sum_{n=1}^{N} I_n p_n(x) \tag{6}$$

Herein, $q(x)$ denotes the true surface charge density, $q_s(\dot{x})$ designates the unknown function, N is the number of sections into which the function is split, I_1 through I_N represent unknown constants, and $p_1(x)$ through $p_N(x)$ are assumed known functions. The summation is approximately equal to $q_s(\dot{x})$. Each $p_n(x)$ is a pulse function, as defined in Equation 7.

$$p_n(x) = \begin{cases} 1, & x_n - \dfrac{\delta}{2N} < x < x_n + \dfrac{\delta}{2N} \\ 0, & otherwise \end{cases} \tag{7}$$

Herein, x_n denotes the nth pulse point.

When this pulse function is incorporated into the integral equation (Equation 5) for anything beyond the limits of $x_n - (\delta/2)$ and $x_n + (\delta/2)$ [$x_n - (\delta/2N)$ and $x_n + (\delta/2N)$], the function disappears; so, the integral is represented by Equation 8.

$$\sum_{n=1}^{N} \frac{I_n}{2\pi\varepsilon_0} \int_{x_n - \frac{\delta}{2N}}^{x_n + \frac{\delta}{2N}} \ln\left(\frac{1}{|x - \dot{x}|}\right) dx \tag{8}$$

Next is the testing stage, in which the summation is expanded with different n's, depending upon the number of sections into which the function is split, a value previously referred to as N. By setting $n = 1,2,3,...,N$, analysts can create an $N \times N$ matrix a in which each row (m) represents the potential on a section and each column (n) represents how that section affects the pulse point at x_m. In the matrix element a_{mn}, if H represents the width of the pulse and w represents the width of the strip, then $a_n = (-w/2) + (n - 1)H$ is the lower limit of the pulse, $b_n = (-w/2) + nH$ is the upper limit of the pulse, and $x_m = (-w/2) + (n - ½)H$, which puts the points in the center of the pulses. The following functions (Equations 9 and 10) are used to calculate the unknown values.

$$\begin{bmatrix} a_{11} & \cdots & a_{1N} \\ \vdots & \ddots & \vdots \\ a_{N1} & \cdots & a_{NN} \end{bmatrix} \begin{bmatrix} I_1 \\ \vdots \\ I_N \end{bmatrix} = \begin{bmatrix} f_1 \\ \vdots \\ f_N \end{bmatrix} \tag{9}$$

$$a_{mn} = \frac{1}{2\pi\,\varepsilon_0} \int_{a_n}^{b_n} \ln\left(\frac{1}{|x_m - \dot{x}|}\right) d\dot{x}, \quad f_m = \text{potential at } x_m = \Phi(x_m) \tag{10}$$

By multiplying the vector $\vec{f}$ by the inverse of the matrix a, one can solve for the unknown I_n's. Problems arise when calculating the integral of the diagonal terms (a_{ii}) due to the singularity at x_m, where the denominator in the integral turns to 0. Gaussian quadrature is used to avoid this singularity by splitting the pulse in half and summing the integrals from both sides. This type of quadrature does not evaluate the integrand at the end points, thereby avoiding this singularity.

The graphs that follow (Figures 4 through 8) represent the results of this problem solved via the numerical method described. Figures 4, 5, and 6 show the results of solving the problem with 100 pulses. Figure 4 shows the data for this problem when the forcing function is $\Phi(x) = 1$. In contrast, Figure 5 shows the results when the forcing function is $\Phi(x) = x$, an odd function. By comparing the two, analysts see that the function is odd when the forcing function is odd and is even when the forcing function is even. This outcome is confirmed by Figure 6, which shows the results for a forcing function of $\Phi(x) = x^2$.

Figures 7 and 8 afford a comparison of the results for similar forcing functions with different numbers of pulses. The curve shown in Figure 7 represents the data for 15 pulses and that depicted in Figure 8 provides the data for 50 pulses. These figures show that the function becomes much smoother as more pulses are used; although, the curve does not become significantly smoother as the number of pulses increases beyond 50.

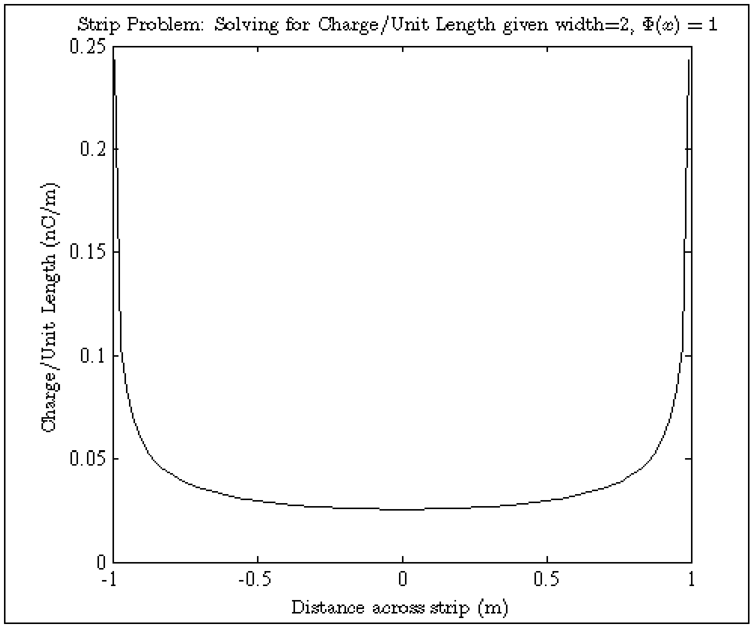

FIGURE 4. Strip Problem Results, Charge Density Across 2-meter-wide Strip, With Even Forcing Function of $\Phi(x) = 1$.

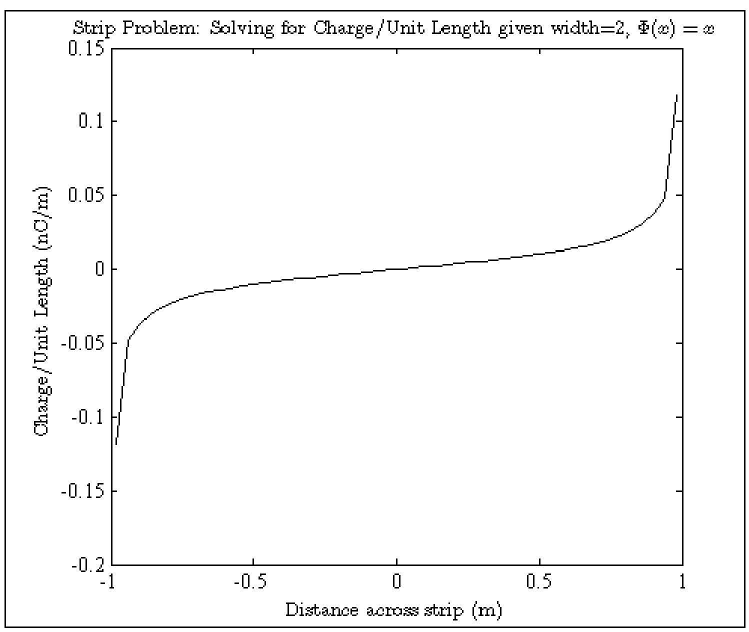

FIGURE 5. Strip Problem Results, Charge Density Across 2-meter-wide Strip, With Odd Forcing Function of $\Phi(x) = x$.

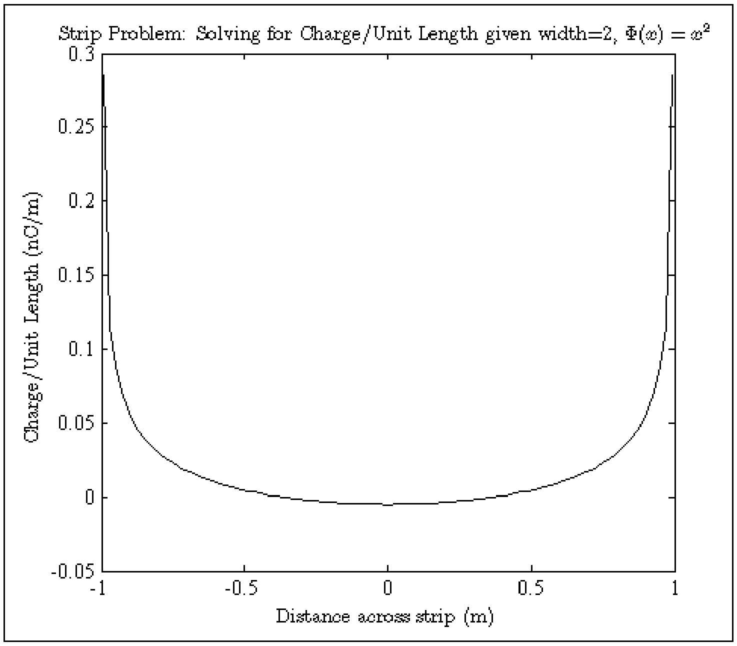

FIGURE 6. Strip Problem Results, Charge Density Across 2-meter-wide Strip, With Even Forcing Function of $\Phi(x) = x^2$.

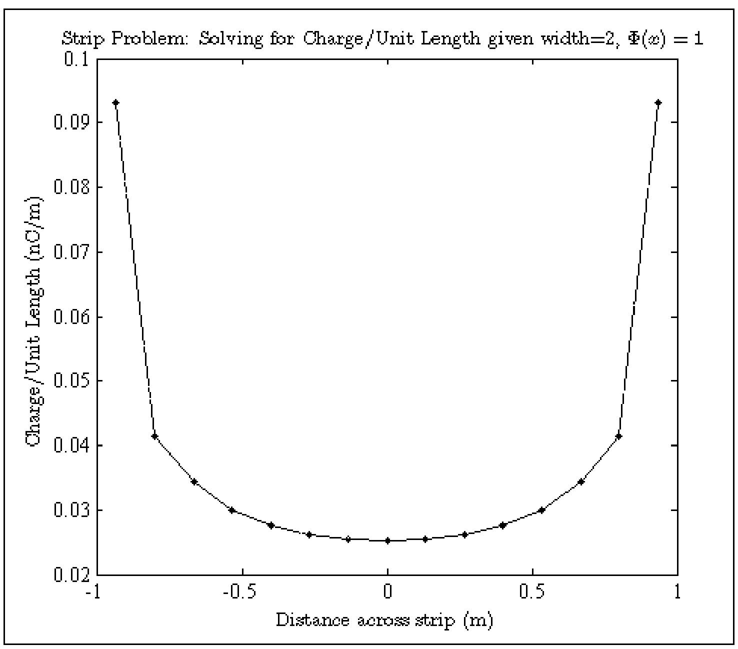

FIGURE 7. Strip Problem Results, Charge Density Across 2-meter-wide Strip. Herein, the number of pulses (N) is 15 and the forcing function is $\Phi(x) = 1$.

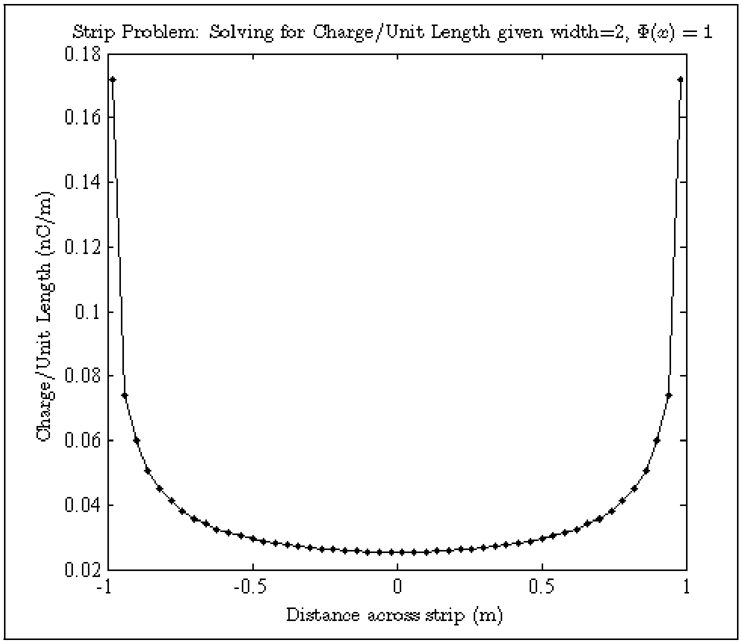

FIGURE 8. Strip Problem Results, Charge Density Across 2-meter-wide Strip. Herein, the number of pulses (*N*) is 50 and the forcing function is $\Phi(x) = 1$.

Another variation on the strip problem involves incorporating two strips (coupled strips) into the equation and adjusting the calculations to reflect the presence of another strip. This addition is first examined as the two strips are aligned along the same axis and are separated only by a small amount of space. In these calculations, the matrix becomes a partitioned matrix and is only symmetric within each portion. The matrix is set up as follows.

$$\begin{bmatrix} \text{effects of A on } \mathbf{A} & \text{effects of B on } \mathbf{A} \\ \text{effects of A on } \mathbf{B} & \text{effects of B on } \mathbf{B} \end{bmatrix}$$

Figure 9 shows the outcome of applying this method to coupled strips that are aligned along the same axis. The figure indicates that, though the strips are not connected, the existence of another set of charges influences the charge distribution.

In another configuration used, the strips were arranged in a cylinder and infinitely small gaps where left where the strips would meet. The data in Figure 10 reflect the outcome of this arrangement, and the figure shows that the singularity that occurs at the edge of the strip is still present, though the direction of the singularity is opposite from strip to strip. This trend is also clear in Figure 11; the data in that figure, which represent the charge density measured around the cylinder, is plotted in two dimensions—radians and charge density.

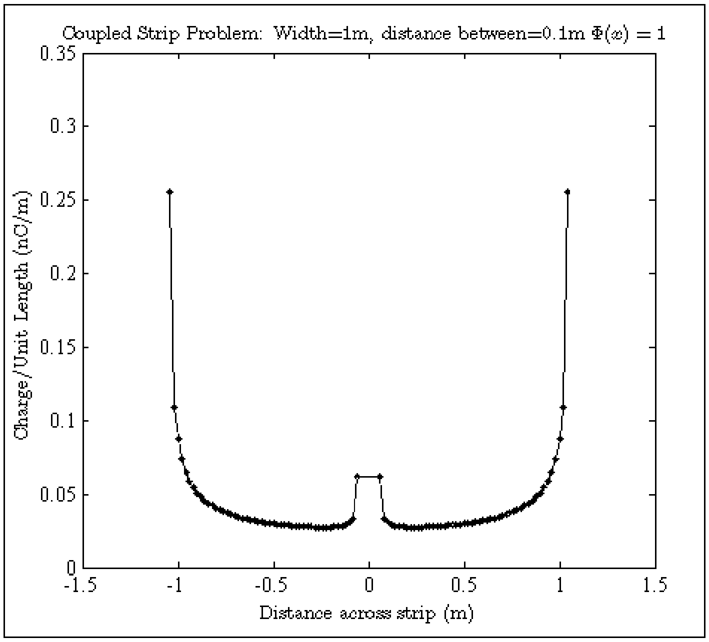

FIGURE 9. Coupled Strip Problem Results, Charge Density Along Coupled 1-meter-wide Strips Aligned on X-axis and Separated by 0.1-meter-wide Space.

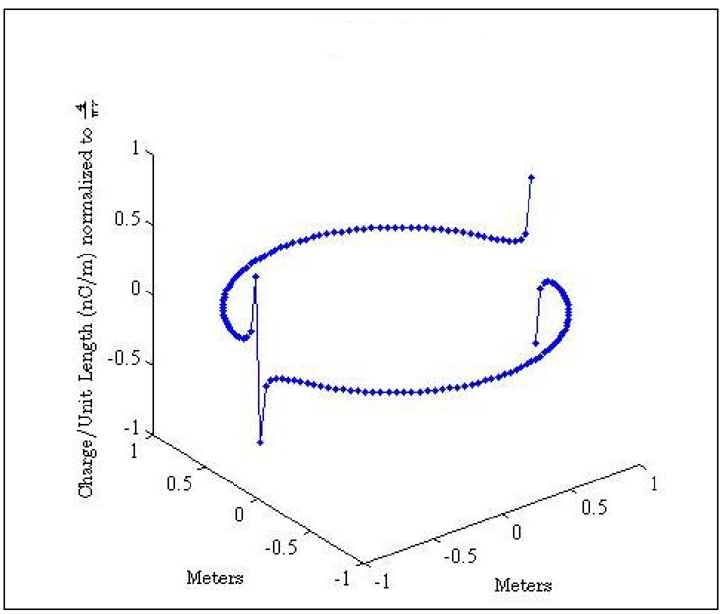

FIGURE 10. Three-dimensional Plot of Charge Density Around Coupled Strips Oriented in Cylindrical Shape With 1-meter Radius.

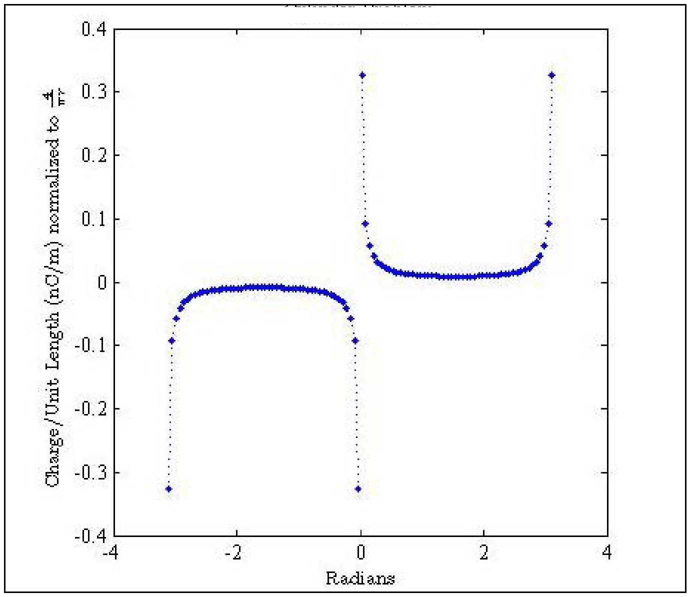

FIGURE 11. Two-dimensional Plot of Charge Density Around Coupled Strips Oriented in Cylindrical Shape With 1-meter Radius.

Yet another variation on this problem is the square cylinder scattering problem in which one strip is shaped into a square-cylinder and excited by an incidental plane wave. Through orientation of the cylinder in such a way that the plane wave is propagating in a direction normal to the axis of the cylinder, the induced surface current and scattered electric field have components only in the direction of the axis of the cylinder. This situation is called transverse magnetic illumination and is solved with an electric field integral equation (EFIE). Because this is a two-dimensional problem, the EFIE is represented by Equation 11.

$$E_z^i(\rho) = \frac{k\eta}{4}\int_C J_z(\rho')H_0^{(2)}\left(k|\rho-\rho'|\right)dl', \quad \rho \in C \tag{11}$$

Herein, E_z^i = designates the z-component of the incidental electric field, ρ is in radians ($|\rho-\rho'|$ (ρ' denotes the source point) is the distance between the points, k is the wavenumber ($2\pi/\lambda$, in which λ is the wavelength), η is the intrinsic impedance (377 ohms for air), C designates an arbitrary closed contour, J_z is the induced current density

(amperes/meter), and $H_0^{(2)}$ is a zero-order Hankel function of the second kind. The distance portion can be rewritten in Cartesian coordinates as Equation 12.

$$|\rho - \rho'| = \left[\left(x_m - x_n - l'\hat{x} \cdot \hat{l}_n \right)^2 + \left(y_m - y_n - l'\hat{y} \cdot \hat{l}_n \right)^2 \right]^{\frac{1}{2}} \tag{12}$$

Herein, x_n, y_n, x_m, and y_m denote Cartesian coordinates that represent the intervals along the circumference, $\hat{x}$ designates the unit vector in the x direction, $\hat{y}$ designates the unit vector in the y direction, l' denotes an arc length variable, and $\hat{l}_n$ represents a unit vector directed along the nth segment.

The diagonal terms are not as easy to handle as in the previous method of moments cases; so, instead, the formula inside the integral is rewritten as Equation 13 to avoid any problems.

$$H_0^{(2)}\left(k|l'|\right) = \left[H_0^{(2)}\left(k|l'|\right) - l + j\frac{2}{\pi}\left[\ln\left(\frac{k|l'|}{2} \right) + \gamma \right] \right] + l - j\frac{2}{\pi}\left[\ln\left(\frac{k|l'|}{2} \right) + \gamma \right] \tag{13}$$

Herein, l designates length; $j^2 = -1$; and γ denotes Euler's constant, approximately 0.5772.

The final factor to consider is the "forcing function" or, here, an incidental plane wave, which is calculated using Equation 14.

$$E_z^i(\rho) = E_0^i e^{jk\left(x\cos\theta^i + y\sin\theta^i\right)} \tag{14}$$

Herein, θ^i is the angle of the incidental plane wave as measured from the x-axis.

Solving for the current by using the method of moments, analysts can determine the distribution of current around the cylinder (see Figure 12). This figure provides the results for only half way around the cylinder, starting at the middle of the side facing the incidental wave. The data indicate that the current is concentrated on the side that comes into contact with the incident wave first. As the reader can see, the singularities occur at the corners (the corners are at pulses 10 and 30). Also apparent is the lack of current on the far side.

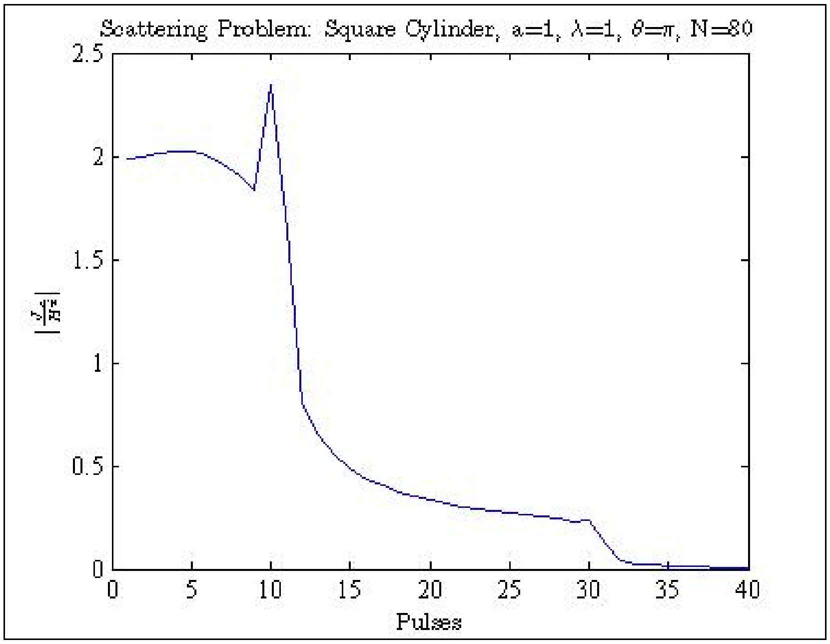

FIGURE 12. Square-cylinder Scattering Problem Results, Normalized Current Density Half Way Around Square Cylinder Excited by Plane Wave Oriented at Angle of π Radians From X-axis.

THIN-WIRE ANTENNA PROBLEM

A wire is deemed thin when, due to the thinness of the wire, one can assume the surface current ($\vec{J}$) is the sum of the interior and exterior surfaces of the cylinder. This assumption is allowable when the thickness of the wire is small in comparison with the wavelength of the incidental wave (λ), typically around 0.01λ. Because the wire is so thin, $\overline{E}^{i}$ is invariant around the cylinder, thereby leaving the only component of $\overline{E}^{i}$ tangential to the surface to be the component in the z direction. In this problem, an inherent assumption is that the antenna is a perfect electrical conductor, thus allowing the boundary condition represented in Equation 15.

$$E_z^s + E_z^i = 0 \tag{15}$$

Herein, E_z^s is the z-component of the scattered electromagnetic field, and E_z^i is the z-component of the incidental electromagnetic field. The antenna is also said to have a radius of a and a height of $2h$. Through derivation, one can generate Equations 16 and 17.

$$E_z^i = \frac{j\omega}{k^2\left(k^2 A_z + \frac{\partial^2 A_z}{\partial z^2}\right)} \tag{16}$$

$$A_z = \frac{\mu}{4\pi}\int_{z=-h}^{h} J_z\left(\dot{z}\right)\int_{\theta=-\pi}^{\pi} \frac{e^{-jkR}}{R} a\, d\theta\, d\dot{z}\,, \tag{17}$$

Herein, ω = frequency; $R = \left|\vec{r} - \vec{r}\,'\right|$; k is the wavenumber, defined as $k = \omega\sqrt{\mu\varepsilon}$, where μ = the permeability of the medium and ε is the permittivity of the medium; A_z = the vector potential; and $j^2 = -1$.

To solve A_z, Equations 18, 19, and 20 are used. Herein, $\dot{z}$ is a variable used to describe a coordinate.

$$K\left(z - \dot{z}\right) = \frac{1}{2\pi}\int_{-\pi}^{\pi} \frac{e^{-jkR}}{R} d\theta \tag{18}$$

$$J_z\left(z\right) = 2\pi a\left(I\left(z\right)\right) \tag{19}$$

$$E_z^i\left(z\right) = j\left(\frac{\eta}{4\pi k}\right)\left(\frac{\partial^2}{\partial z^2} + k^2\right)\int_{-h}^{h} I\left(\dot{z}\right) K\left(z - \dot{z}\right) d\dot{z} \tag{20}$$

If $f\left(z\right) = \int_{-h}^{h} I\left(\dot{z}\right) K\left(z - \dot{z}\right) d\dot{z}$, then Equation 21 applies.

$$E_z^i\left(z\right) = j\left(\frac{\eta}{4\pi k}\right)\left(\frac{\partial^2}{\partial z^2} + k^2\right) f\left(z\right) \tag{21}$$

The solution to this differential equation is in the form of Equation 22.

$$f\left(x\right) = f_h\left(x\right) + f_p\left(x\right) \tag{22}$$

Herein, f_h is the homogeneous solution and f_p is the particular solution.

Solving as a differential equation results in Hallén’s equation (Equation 23).

$$E_z^i(z) = j\left(\frac{\eta}{4\pi k}\right)\left(\frac{\partial^2}{\partial z^2} + k^2\right)\int_{-h}^{h} I(\dot{z})K(z-\dot{z})\,d\dot{z}$$
$$= C\cos kz + B\sin kz + v(z),\, z \in (-h,h)$$

$$v(z) = \frac{1}{k}\int_0^z E_z^i(\dot{z})\sin k\left(\ \left|z-(z\right|\ )\right)d\dot{z}\text{ , with } I(\pm h) = 0 \tag{23}$$

This equation can be solved by using the method of moments. For an antenna problem, E_z^i is replaced by $V\delta\left(z - z_g\right)$ (the Dirac delta function), *V* denotes the delta function "strength," and the equation is solved by using pulse expansion and testing for a current fed at z_g. Based on the assumption that the forcing function is fed at z_0, the delta function is evaluated at z_0. The first step is to expand with pulses of uniform width Δ and approximate *I(z)* via Equation 24.

$$I(z) = \sum_{n=1}^{N} I_n \Pi_n(z) \tag{24}$$

I_n's are unknown complex constants and Equation 25 applies.

$$\Pi_n(z) = \begin{cases} 1, & \text{if} \quad z_n - \dfrac{\Delta}{2} < z < z_n + \dfrac{\Delta}{2} \\ 1, & \text{otherwise} \end{cases} \tag{25}$$

Half of a pulse is placed at either end of the antenna and given a height of zero to account for the constraint of 0 current at $+h$ and $-h$. Then, enforcing the resulting equation at the matching points (z_m) results in Equation 26.

$$v(z_m) = j\left(\frac{\eta}{4\pi k}\right)\int_{-h}^{h}\sum_{n=1}^{N} I_n\Pi_n(\dot{z})K(z_m - \dot{z})\,d\dot{z} - C(\cos kz_m) - B(\sin kz_m) \tag{26}$$

Herein, $m = 0,1,2,\ldots N + 1$.

This equation can be rewritten when considering the delta function as Equations 27 and 28 to derive Equations 29, 30, and 31.

$$V_m = v_m(z) = \frac{1}{k}\int_0^{z_m} E_z^i(\dot{z})\sin k\left(\left|z_m - \dot{z}\right|\right)d\dot{z} = \frac{1}{k}\sin k\left(\left|z_m\right|\right) \tag{27}$$

$$\sum_{n=1}^{N} I_n Z_{mn} - C\cos kz_m - B\cos kz_m = V_m, \qquad m = 0,1,2,\ldots N+1 \tag{28}$$

$$z_m = -h + m\Delta, \qquad Z_{mn} = j\frac{\eta}{4\pi k}\int_{z_n-\frac{\Delta}{2}}^{z_n+\frac{\Delta}{2}} K\left(z_m - \dot{z}\right) d\dot{z}, \tag{29}$$

$$K\left(z-\dot{z}\right) = \frac{1}{2\pi}\int_{-\pi}^{\pi}\frac{e^{-jkR}}{R}d\theta,\ R = \left|\vec{r}-\vec{r}'\right| = \sqrt{\left(z-\dot{z}\right)^2 + 4a^2\sin^2\frac{\theta}{2}}, \tag{30}$$

$$\Delta = \frac{2h}{N+1} \tag{31}$$

There are now N + 2 equations (including the pulses at either end) and N+2 unknowns (including B and C), which can be solved using linear algebra. By setting up the following matrices, one can solve for the unknown I's, as well as C and B.

$$\left[\left(-\cos\left(kz_{\downarrow}0\right) \,\&\, z_{\downarrow}01 \,\&\, \ldots \,\&\, z_{\downarrow}0N \,\&\, -\sin\left(kz_{\downarrow}0\right) @ -\cos\left(kz_{\downarrow}1\right) \,\&\, z_{\downarrow}11 \,\&\, \ldots \,\&\, Z_{\downarrow}1N \,\&\, -\sin\left(kz_{\downarrow}1\right) @ \vdots \,\&\, \vdots \,\&\, \ddots \,\&\, \vdots \,\&\, \vdots @ -\cos\left(kz_{\downarrow}N\right) \,\&\, z_{\downarrow}\left(N,1\right) \,\&\, \ldots \,\&\, Z_{\downarrow}NN \,\&\, -\sin\left(kz_{\downarrow}N\right) @ -\cos(kz_{\downarrow}\left(n+1\right)\right)\right]$$

The rows (m) each represent a point on the wire, while the columns (n) each represent the corresponding pulse on the wire and the way in which the pulse affects the other points.

The graphs provided in Figures 13 and 14 show the different variations of this problem. Plotted in Figure 13 is the magnitude of the complex vector when λ = 1 meter, N = 53, a = 0.007022 meter, and the length of the rod is $^{\lambda}/_{2}$. Figure 14 shows the change in the current when the size of the radius (a) is decreased.

Figure 15 shows the distribution of current changes as the location of feed input, which was previously held at z = 0, is moved. These data indicate how the current changes as it is moved repeatedly three pulses away. Here, the asterisks (*) represent the location of input, the dotted lines designate the imaginary parts, and the solid lines signify the real parts. Figure 16 shows the plot of the magnitude of the vector.

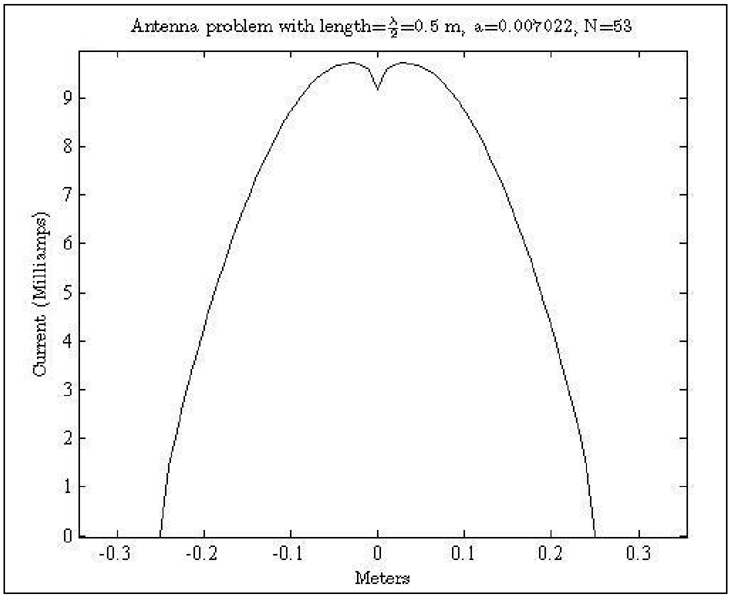

FIGURE 13. Antenna Problem Results, Current Along Thin-wire Antenna (Length = λ/2).

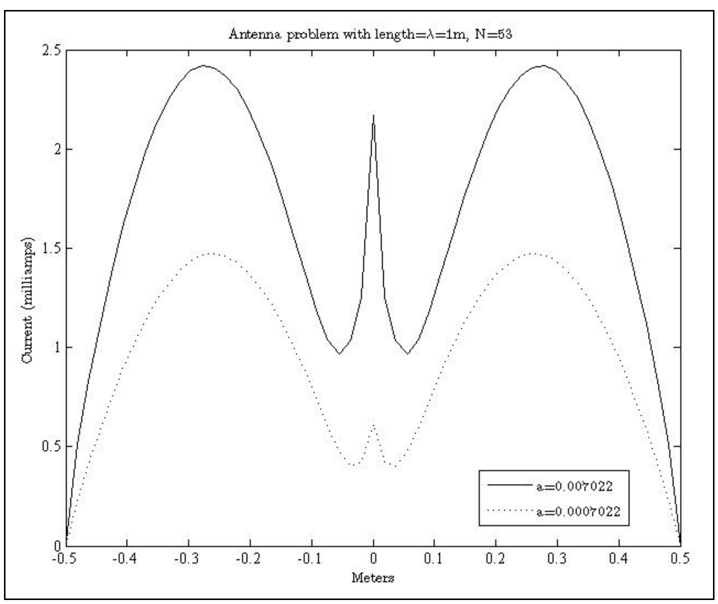

FIGURE 14. Antenna Problem Data Showing Differences Resulting From Changes in Size of Radius (*a*), Current Along Thin-wire Antenna (Length = λ).

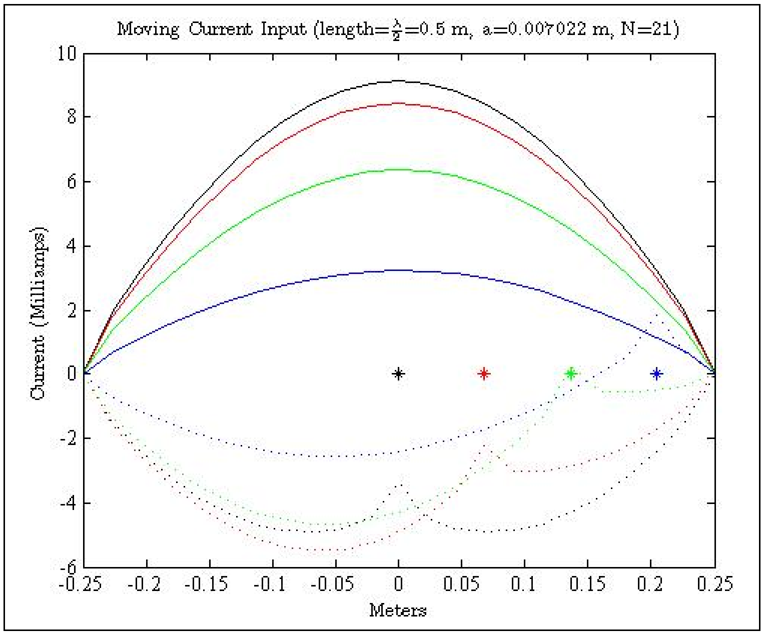

FIGURE 15. Antenna Problem Results Showing Effect of Varying Input Location of Current Along Thin-wire Antenna.

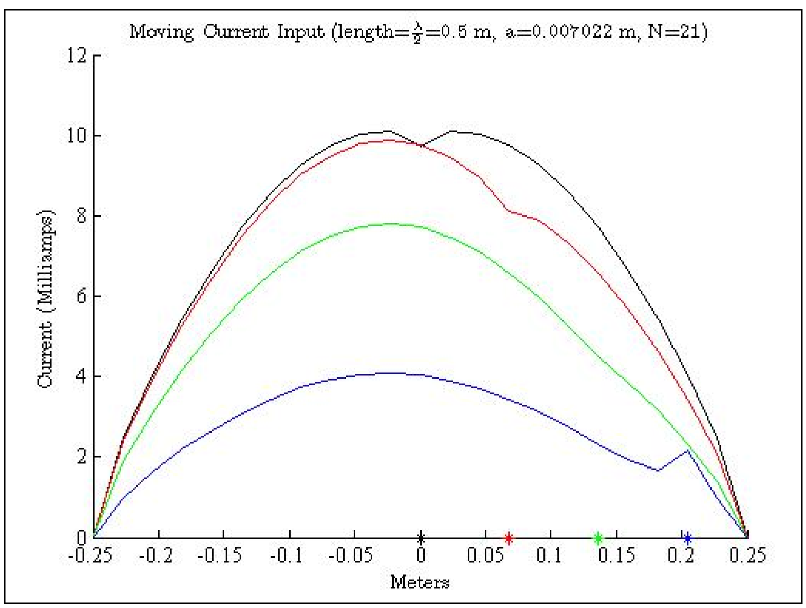

FIGURE 16. Antenna Problem Results, Magnitude of Current Vector. Graph shows effect of varying current input location along thin-wire antenna.

The graphs in Figure 17 provide a comparison of the effect that different lengths of wire have on the resultant data. These graphs, plots of the magnitude of the complex vector, show the sine curves for the input force. As the reader can see, the current of this wire is dependent upon its length.

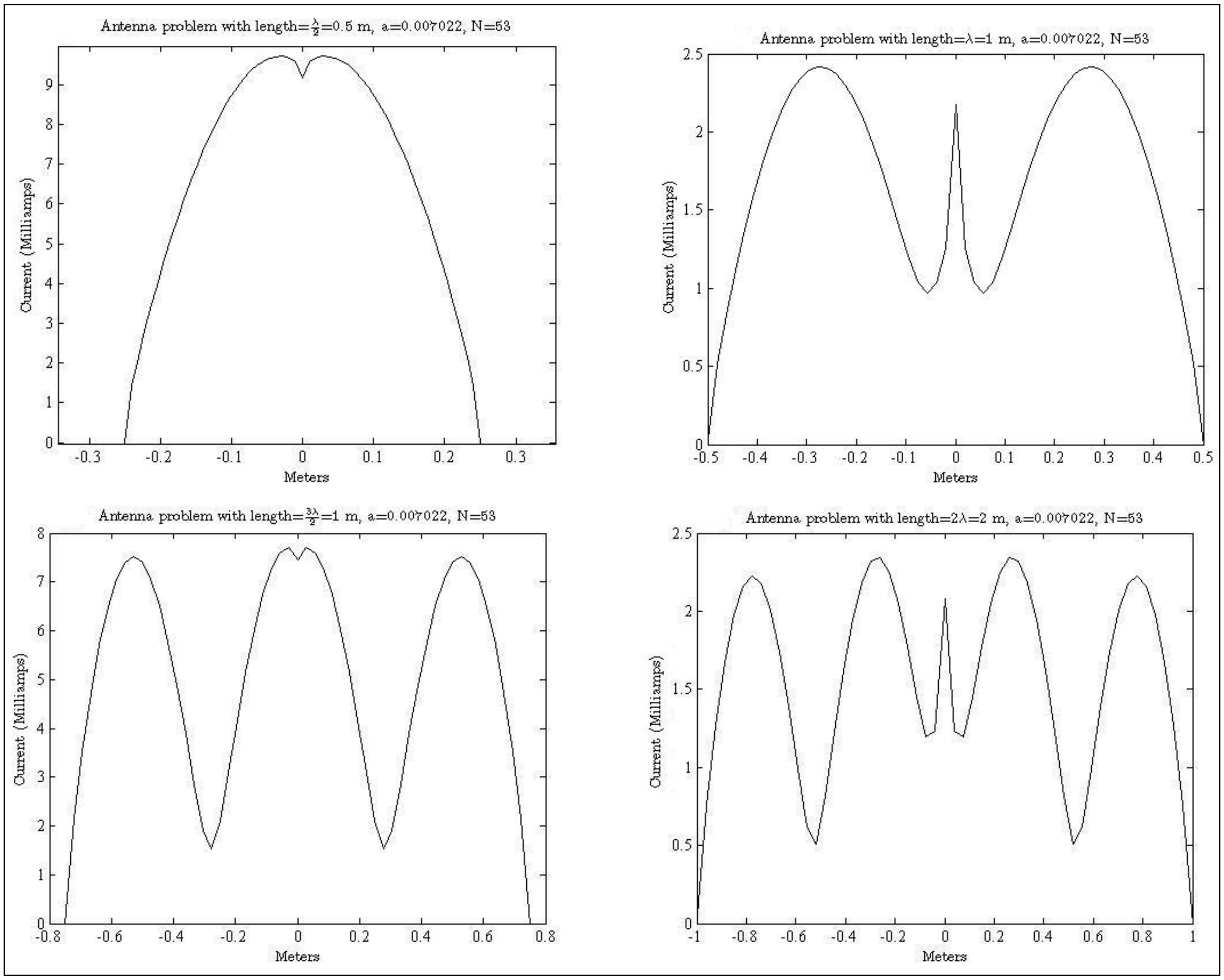

FIGURE 17. Antenna Problem Results for Different Lengths of Thin-wire Antenna. Graphs provide a comparison to demonstrate the effect on the current by varying the thin-wire antenna length (0.5, 1, 1.5, and 2 meters).

Changing the force acting upon the antenna to an incidental wave results in the problem becoming a scattering problem. Figure 18 shows the distribution when the wire length is $\lambda/4$, and Figure 19 shows the scattering distribution when the wire is $\lambda/2$.

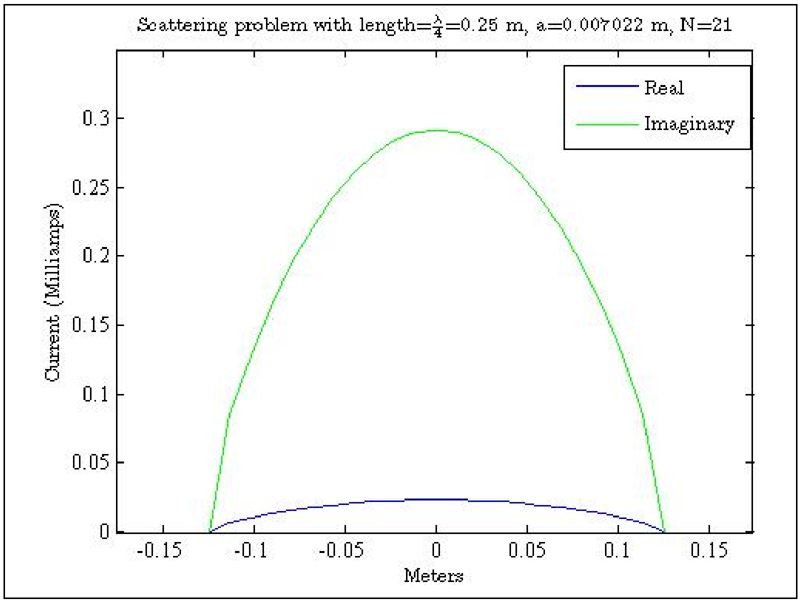

FIGURE 18. Scattering Problem Results, Current Along Thin-wire Antenna (Length = λ/4) Excited by Incidental Plane Wave.

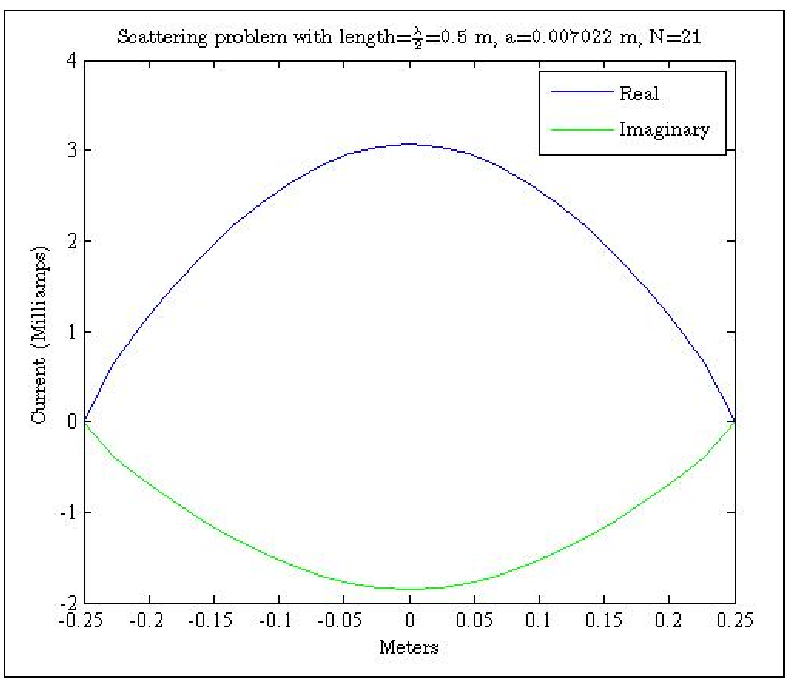

FIGURE 19. Scattering Problem Results, Current Along Thin-wire Antenna (Length = λ/2) Excited by Incidental Plane Wave.

CONCLUSION

This document describes the author's experience as an intern at the NAWCWD in learning the basics of electrostatics and electrodynamics, as well as how to approach computational models in physics. Herein, she discusses the models and methods that she adopted to solve various fundamental problems applicable to these fields. Moreover, the author shows how to use the method of moments to calculate the charge density across a strip and the current along a thin-wire antenna.

NOMENCLATURE

ε_0	permittivity of free space (8.854223×10^{-12} Farads/meter)
ε	permittivity of a medium
μ	permeability of a medium
λ	charge per unit length wavelength
ϕ	electric potential
$\Phi(x)$	forcing function
δ	width of strip in strip problem
ρ	distance between the points
$\lvert\rho - \rho'\rvert$	ρ in radians
η	intrinsic impedance
γ	Euler's constant, approximately 0.5772
θ^i	angle of incidental plane wave as measured from x-axis
a_{ii}	i'th diagonal term of matrix a
a_{mn}	(m,n)'th element of matrix a
a_n	lower limit of pulse n
b_n	upper limit of pulse n
C	an arbitrary closed contour
E	electric field
H	width of pulse
$H_0^{(2)}$	zero-order Hankel function of the second kind
I_n	unknown constants
j	the square root of -1, i.e. the imaginary unit
$\vec{J}$	surface current
J_z	induced current density (amperes/meter)
k	wave number ($2\pi/\lambda$, in which λ is the wavelength)

l	length
$\hat{l}_n$	an arc length variable
l_n	a unit vector directed along the nth segment
N	number of pulses used in a method of moments solution
P	a point at which electric field strength is observed
ρ	an arbitrary point along C
ρ'	source point
$\vec{\rho}$	location at which potential is observed
$\dot{\vec{\rho}}$	location of a charge
$p_n(x)$	pulse functions
q	electric charge
q_i	source charge
$q_i, \ldots, q_n$	charges
q_L	line charge density
$q(x)$	true surface charge density
$q_s(\dot{x})$	potential across surface
r	distance between the point P and source charge q_i (Equation 1) distance between dl and P (Equation 2)
$\hat{r}$	unit vector between point P and source charge q_i (Equation 1) unit vector between dl and P (Equation 2)
NAWCWD	Naval Air Warfare Center Weapons Division
V	Dirac delta function "strength"
w	width of strip
x	horizontal direction in two-dimensional space one of the three fundamental directions in three-dimensional space x-component of $\vec{\rho}$
$\dot{x}$	x-component of $\dot{\vec{\rho}}$
$\hat{x}$	unit vector in the x direction
x_m	x-coordinate of an arbitrary point m along C
x_n	x-coordinate of an arbitrary point n along C
y	vertical direction in two-dimensional space one of the three fundamental directions in three-dimensional space
$\hat{y}$	unit vector in the y direction
y_m	y-coordinate of an arbitrary point m along C
y_n	y-coordinate of an arbitrary point n along C
z	one of the three fundamental directions in three-dimensional space
$\dot{z}$	variable used to describe a coordinate

INITIAL DISTRIBUTION

1 Defense Technical Information Center, Fort Belvoir, VA

ON-SITE DISTRIBUTION

20 Code 4L4100D
Halterman, K.
2 Code 4L6100D (Technical Library)
1 Code 4L6200D